RSC Advances

Depollution of Syringic Acid aqueous solutions by electrochemical oxidation using high oxidation power anodes

Journal:	*RSC Advances*
Manuscript ID	RA-ART-05-2016-012079.R2
Article Type:	Paper
Date Submitted by the Author:	19-Jul-2016
Complete List of Authors:	dridigargouri, olfa; Ecole Nationale d\'Ingenieurs de Sfax, ; kallel, souhel; enis abdelhadi, ridha; enis
Subject area & keyword:	Electrochemistry < Physical

Depollution of Syringic Acid aqueous solutions by Electrochemical Oxidation using high oxidation power anodes

O. Dridi Gargouri*, S. Kallel Trabelsi, R. Abdelhèdi,

U.S. Electrochemistry and Environment, National Engineering School, BP 1173, 3038 Sfax, University of Sfax, Tunisia

Corresponding author:

Dr. Olfa DRIDI GARGOURI

Laboratoire d'Electrochimie et Environnement, Ecole Nationale d'Ingénieur de Sfax, BP 1173, 3038 Sfax. Université de Sfax. Tunisie.

E-mail : olfadridigargouri@yahoo.fr

Abstract

The anodic oxidation of Syringic Acid aqueous solutions has been comparatively studied using lead dioxide (PbO_2) and boron-doped diamond (BDD) anodes in an electrolytic cell. The influence of several operating parameters such as current density and SA concentration on the performance of both systems has been investigated and the energy consumption has been also evaluated. Galvanostatic electrolyses always cause concomitant generation of hydroxyl radical that leads to the SA destruction. The efficiency of the electrochemical process increases at lower current density and higher SA initial concentration while it decreases with the COD removal progress.

The performance of the BDD anode is always better than that of PbO_2, requiring shorter electrolysis time to reach overall mineralization, due to the high amounts of effective hydroxyl radicals generated from water oxidation at each anode, which lead to a higher current efficiency and a lower specific energy consumption when BDD anode was used. A possible reaction mechanism for SA oxidation with $^{\bullet}OH$ was proposed. The kinetics decays for the SA degradation on PbO_2 anode follows a pseudo-first order reaction with a rate constant 8.3 10^{-3} min^{-1} for j_{app} value 15 mA cm^{-2}.

Keywords: Syringic acid; Wastewater treatment, Hydroxyl radicals, Electrochemical Oxidation; lead dioxide; Boron-Doped Diamond

1. Introduction

Industrial effluents which contain toxic and non-biodegradable species cause serious environmental problems due to, on the one hand, the absence of efficacious treatment processes and, on the other hand, the legislation severity of tolerated norms. Among these effluents, olive mill wastewater (OMW), which has a high polluting organic load, due to a high content of organic substances, including phenolic compounds such as tyrosol, coumaric acid, vanillic acid, syringic acid,…[1–2]. These compounds are major contributors to the toxicity and the antibacterial activity of OMW, which limits its microbial degradability. Taking into account the toxicity of these compounds in the OMW, Advanced Oxidation Processes (AOPs) are reported to be a promising alternative to remediate effluents which cannot be treated by conventional biological treatments. Recently, AOPs have proved as both an efficient and viable alternative for the treatment of wastewaters. In fact, this is due to its unique ability to oxidize or reduce contaminants in the water near the well-controlled electrode[3] and its attractive characteristics, such as versatility, energy efficiency, amenability of automation and environmental compatibility (free-chemical reagents). The electrochemical methods are environmentally friendly since they have various advantages, among which wide application, simple equipment, easy operation, no consumption of chemical, lower temperature requirements and lack of sludge formation can be mentioned[4]. Most AOPs involve the in situ generation, at anode surface by water discharge, of highly reactive species such as hydroxyl radicals $^{\bullet}OH$ (Eq.1). These later are able to oxidize a wide range of chemicals[4–6].

$$H_2O \rightarrow {}^{\bullet}OH + H^+ + e- \quad (1)$$

Hydroxyl radicals $^{\bullet}OH$ is the second most strong oxidant known after fluorine and has a very high standard potential ($E^0(^{\bullet}OH/ H_2O)$ = 2.80 V vs. NHE) that makes it able to non-

77 selectively react with organic pollutants giving dehydrogenated or hydroxylated derivatives
78 up to overall mineralization, i.e., total conversion into CO_2 and inorganic ions.
79 Over the past years, the application of anodic oxidation to water remediation has received
80 great attention owing to the use of special electrodes with high oxygen over-potential anodes,
81 such as lead dioxide PbO_2 [4–7] , Tin dioxide SnO_2[7], and boron-doped diamond BDD[7–11].
82 Some previous studies have reported that PbO_2 and BDD have high oxidation power and are
83 able to generate highly reactive physisorbed $^{\bullet}OH$ from reactions (1) thus leading to overall
84 combustion of organic compounds such as pesticides[6,8], synthetic organic dyes[10,12] and
85 phenolic compounds[5,13].

86 In this reaserch, Sringic Acid (SA) was selected as a model molecule representative of
87 phenolic compounds in the OMW. Due to the high toxicity of this compound, effective
88 treatment methods are needed for its degradation. Until now, SA degradation has been studied
89 by ozonation[14], Fenton[15], photo-catalytic[16], and photo-Fenton process[17]. In another way, it has
90 been reported in our previous research that anodic oxidation of SA was applied for
91 electrosynthesis of high add value product[18].

92 Thus, considering that BDD and PbO_2 electrodes have shown good electro-catalytic
93 activity towards the electro-oxidation of organics compound, the aim of the present work is to
94 study the decontamination of acidic SA solutions by electrochemical oxidation under different
95 experimental conditions. This work was also focused on the kinetics analysis, the
96 identification of the degradation intermediates and to propose a mineralization pathway for
97 SA.

98 2. Experimental section

99 Reagents and chemicals

In this work, all solutions were prepared in the laboratory with ultrapure water. SA was purchased from Aldrich and was used as received. For most of the experiments, the initial pH was 1.8 adjusted using a prepared 1 mol L^{-1} sulfuric acid.

Electrolytic cells

All electrolyses were conducted in an open, divided and thermostated cylindrical glass cell (150 ml) under galvanostatic conditions using a DC power supply. The anode was either a 4 cm^2 BDD film (1300 ppm of B and thickness 1.33 μm) deposited on single crystal p-type Si(100) wafers (conductivity 0.1 Ω^{-1} cm^{-1}) supplied by Adamant Technologies or a 4 cm^2 Ta/PbO_2 placed in front of the cathode. The experimental details for the preparation of Ta/PbO_2 were described in our previous research work[6]. In all trials the cathode was a graphite bar (φ = 1 cm; L = 6 cm) placed in a porous ceramic cylinder (Norton, RA 84) containing 1 mol L^{-1} sulfuric acid solution.

Analytical procedures

During the experiments, samples were drawn in the bulk of the reservoir at different times and analysed. The SA oxidation was followed by the Chemical Oxygen Demand (COD), reversed-phase HPLC and Liquid chromatography–mass spectrometry (LC–MS) analysis.

The COD concentration was measured colorimetrically using a Shimadzu spectrophotometer UV-V (model 1650 PC). The experimental details for COD analysis were described in our previous research work[6].

These data allowed calculating the current efficiency (CE, in %) for each treated solution at a given electrolysis time from the Equation (2):

$$CE = \frac{(COD_0 - COD_t)}{8I\Delta t} FV \times 100 \quad (2)$$

where COD_0 and COD_t are Chemical Oxygen Demands (g O_2 L^{-1}) before electrolyses and at time t (s) respectively, F is the Faraday constant (96487 C mol^{-1}), V is the solution volume (L) and I is the applied constant current (A).

The specific energy consumption (E_{sp}) expressed in KWh (kg COD)$^{-1}$, is the energy used to remove a unit mass of COD from wastewater and can be calculated using the following relation ship[7]:

$$E_{sp} = \frac{FU_c}{8CE3600} \quad (3)$$

where U_c is the cell potential (V), 8 is the equivalent mass of oxygen (g eq^{-1}).

The experimental details for Liquid chromatography–mass spectrometry (LC–MS) of the SA solution after 240 min treatment on PbO_2 anode were described in our previous research work[18].

The SA quantification and its oxidation products during electrolysis were made by high-performance liquid chromatography using a Perkin Elmer 200 series HPLC apparatus. The products formed are separated on a C_{18} column and then analyzed quantitatively using UV–V detector measuring the optical density at 220 nm during the first 5 minute, after that at 270 nm. The mobile phase was a mixture of acetonitrile and 5×10^{-2} mol L^{-1} sulfuric acid with the percentage by volume of acetonitrile varying linearly with time as follow: from 10 to 25% for the first 25 min then from 25 to 80% up to 35 min and finally from 80 to 100% up to 45 min. The mobile flow rate was fixed at 1 mL min^{-1}.

3. Results and discussions

Comparative degradation of SA solutions

A series of electrolyses was carried out in order to study the influence of experimental parameters, such as current density, and SA concentration on the mineralization power of electrogenerated oxidants BDD ($^{\bullet}OH$) and PbO_2 ($^{\bullet}OH$). Fig. 1 presents the COD–times and

COD–Q plots obtained for anodic oxidation of 2 mmol L^{-1} SA (COD_0 = 540 mg O_2 L^{-1}) with BDD or PbO_2 anodes at 8, 15, 60 and 120 mA cm^{-2} and at 30 °C.

Fig. 1(a_1) and (b_1) show, that the COD removal rate is faster, when j_{app} increased from 8 to 60 mA cm^{-2} when the SA oxidation were carried out using PbO_2 or BDD anode, respectively. For example after 360 minutes of SA electrolysis, COD is reduced by about 50, 70 and 80 % using PbO_2 at 8, 15 and 60 mA cm^{-2} respectively. However it decays much more rapidly up to 60%; 80% and 100% for the same j_{app} values when the BDD anode is used instead. This behavior can be explained by the greater generation of reactive BDD ($^{\bullet}OH$) and PbO_2 ($^{\bullet}OH$) when j_{app} increased. In the same context, the COD removal rate with consumed specific charge (Fig. 1(a_2) and (b_2)) decreases with rising j_{app}. For instance, a COD reduction by 50% required the consumption of a specific charge of about 1.3, 1.6, 5 and 6.5 using PbO_2 anode at 8, 15, 60, and 120 mA cm^{-2} respectively (Fig. 1(a_2)). A similar behavior was also observed in the tendency of COD-Q plots presented in Fig. 1(b_2)) when BDD was used. In fact, the specific charge consumption of about 2.4 A h L^{-1}, causes a reduction of COD removal from 85 to 62% for 8 and 60 mA cm^{-2} respectively. Nevertheless, above 60 mA cm^{-2}, we can observe a different behavior to that presented in the case of PbO_2. At high current density (120 mA cm^{-2}), the COD removal rate was later than at 60 mA cm^{-2} (Fig. 1(b_1)). In addition, the consumption of the same specific charge (2.4 A h L^{-1}) reduced significantly the COD removal from 62% to 30% for 60 and 120 mA cm^{-2} respectively. This result could be explained by the loss of hydroxyl radicals (($^{\bullet}OH$)) under the secondary reaction (Eq. 4).

$$2\ ^{\bullet}OH_{ads} \rightarrow \tfrac{1}{2}\ O_2 + H_2O \qquad (4)$$

In order to explain the influence of SA concentration on the oxidation ability of the BDD and PbO_2 anodes, experiments were performed with four different initial COD solutions viz 136, 280, 540 and 1100 mg O_2 L^{-1} in 0.5 M H_2SO_4 at pH 1.8, current density 15 mA cm^{-2} and temperature 30 °C. The COD-Q plots thus obtained for both anodes used are shown in Fig. 2. This latter show that the total mineralization of SA was attained only for lowers

concentrations (from 136 to 540 mg O_2 L^{-1}) during the maximum electrolysis time, but high initial SA contents (1100 mg O_2 L^{-1}) undergo incomplete mineralization. This result can be interpreted by the low reactivity of hydroxyl radicals BDD ($^{\bullet}OH$) or PbO_2 ($^{\bullet}OH$) generated in these condtions to degrade high organic matter quantity. On the other hand, Fig. 2 shows that mineralization rate increases with the initial SA concentration. For instance, after consumption of a specific charge of about 1.8 A h L^{-1}, the amount of degraded organic matters with BDD ($^{\bullet}OH$) is equal to 129; 270; 378 and 650 mg O_2 L^{-1} for initial COD of 136; 280; 540 and 1100 mg O_2 L^{-1}, respectively. This trend can be explained by the increasing of the rate of mass transfer of SA and its oxidation products to the anode causing their faster reactions with greater amounts of $^{\bullet}OH$, thus decreasing the loss of this radical by the secondary reaction (Eq. 4). A similar behavior was also observed in the tendency of COD-Q plots presented in Fig. 2(a) when PbO_2 was used.

In conclusion, the above results illustrate the better performance observed on BDD than on PbO_2 towards the completely mineralization of SA (COD_0 = 540 mg O_2 L^{-1}) traeted at 30 °C and at 15 mA cm^{-2}. Fig. 3 clearly shows that BDD anode enable significantly faster COD removal than PbO_2. In fact, the COD removal after consumption of a specific charge of about 4 A h L^{-1} during electrolysis on PbO_2 and BDD are respectively equal to 74% and 97%.

The greater oxidation ability of BDD illustrates the high reactivity of hydroxyl radicals electrogenerated on this electrode. These radicals weakly bonded on the BDD surface are available to diffuse and react with organic matter into the solution. In addition, it has been reported that the sp^3 (diamond)/sp^2 (graphite) ratio has an important role in the electrochemical properties of boron-doped diamond electrodes towards electro-oxidation of organic compounds. The sp^2-carbon impurities affects the non-active nature of BDD, promoting important variations on the degradation pathway followed during electro-oxidation of organic compounds as well as production of hydroxyl radicals $^{\bullet}OH$[19].

Current efficiency and energy consumption

From the above findings, it can be reported that the SA mineralization at anodes with high oxygen over-potential, leads to the total destruction of the molecule and the formation of CO_2 as final product. Thus the over all mineralization reaction can be written as follows:

$$C_9H_{10}O_5 + 13H_2O \rightarrow 9\ CO_2 + 36\ H^+ + 36\ e- \quad (5)$$

This reaction shows that 36 electrons are involved in oxidatin a SA molecule completely into CO_2. Generally current efficiency is an important issue in electrochemical treatment, due to the relatively high costs of electric power. Selected values of current effenciency thus obtained are collected in Table 1. In both cases studied, a dramatic decay in CE can be observed during anodic oxidation of SA for all j_{app} values. For example, 68%, 63%, 23% and 18% efficiency is found at the beginning of the electrolysis with PbO_2 anode for 8, 15, 60 and 120 mA cm^{-2} respectively, whereupon decaying up to 65%, 38%, 11% and 6% after 480 minutes of electrolysis. A similar behavior was also observed in the tendency of CE presented in table 1 when BDD was used. This behavior can be explained by the progressive formation of short carboxylic acids that are more difficult to be oxidized with $^{\bullet}OH$. However, the current efficiency always decreases with increasing j_{app} from 8 to 120 mA cm^{-2}, because this radical is more rapidly oxidized to O_2 in accordance with the secondary reaction (Eq. 4).

The initial concentration of pollutants is also an important parameter in wastewater treatment. Fig. 4 shows the effect of the initial concentration of SA on the current effenciency during electrolysis on PbO_2 or BDD anodes using a current density of 15 mA cm^{-2}. As can been see, in both cases studied, that at the beginning of electrolysis of concentrated SA solution (COD_0 = 1100 mg O_2 L^{-1}), the CE is 100%, but it is low for weak SA solution. The CE value rises from 67% to 100% and from 53 to 100 % at the beginning of SA electrolyses with BDD or PbO_2 respectively, starting from 136 to 1100 mg O_2 L^{-1} COD. This result can be explained in terms of mass transfer limitations assuming that both direct oxidation and mediated oxidation on the BDD or PbO_2 surface by hydroxyl radicals and other electro-

generated oxidants ($S_2O_8^{2-}$ from the supporting electrolyte H_2SO_4) contribute in the electrochemical process[7]. These compounds are produced by anodic oxidation of sulfate ions present in the solution according to the following equation:

$$2SO_4^{2-} \rightarrow S_2O_8^{2-} + 2e^- \quad (6)$$

In the same context, it has been recorded, that when anodes with high oxygen evolution overpotential are used, organic pollutants can be efficiently removed by hydroxyl radicals electro-generated by water discharge. However, a positive contribution of these chemicals is also foreseen during the final treatment step, when oxygen is produced as secondary reaction. The presence of these strong oxidants in wastewater bulk avoids mass-transfer limitation and increases process efficiency[7].

For large industrial application it is also very important to estimate the treatment costs through the variation of specific energy consumption, calculated from Eq. (3), required as a function of the COD removal percentage for all experiments carried out with PbO_2 or BDD anodes. The main factor affecting this parameter is the applied current density, since an increase in j_{app} causes a great increase in voltage. Table 1 show that BDD consumed less energy than PbO_2, because BDD has higher oxidation rate due to its higher overpotential for oxygen evolution. As can be also observed that, for both AO processes, the energy consumption (E_{sp}) increases with j_{app} and with COD removal. The energy consumption tendence with COD removal can be related to the gradual formation of more refractory products, such as carboxylic acids which are hardly oxidizable intermediates on one hand[20] and to the development of the secondary reaction (Eq. 4) on the other hand. Nevertheless, it is easy to treat carboxylic acids by biological means[21]. So, the electro-oxidation can be used as an economically adequate way for a pre-treatment of the wastewater followed by biological treatment. The increase of the energy consumption is so in accordance with the fall of current efficiency, previously observed.

Identification and time-course of intermediates for SA degradation

From the above findings presented, SA oxidation with BDD or PbO_2 anodes leads to a completely non-selective and highly efficient oxidation of the initial pollutant and its oxidation intermediates. However, the degradation of the TOW at the BDD anode provided higher oxidation rate than the PbO_2 anode for the same operating conditions. For this reason, we are interested in this part to follow the aromatics intermediates and carboxylic acids produced during SA degradation with PbO_2 at 15 mA cm^{-2}.

LC–MS analysis of the SA solution treated 240 min with PbO_2 revealed the formation of two aromatic intermediates, 3-O-methylgallic acid ($MS^1[M-H]^-$ at m/z 183 (Fig.5a); MS^2 at m/z 168, 139 and 124 (Fig. 5b)) and 2,6 dimethoxybenzoquinone ($MS^1[M+H]^+$at m/z 169 (Fig.5c); MS^2 at m/z 153, 134, 124 and 97 (Fig. 5d)). These by-products were confirmed in the reversed-phase HPLC chromatograms of the same treated solutions (Fig. 6), which displayed two well-defined peaks related to 3-O-methylgallic acid at t_r = 4.1 min and 2,6 dimethoxybenzoquinone at t_r = 8.1 min. This latter, was identified from comparison of her tr-value with authentic standards. However, by comparison of chemical structure and polarity of 3-O-methylgallic acid with SA, 3-O-methylgallic acid is elueted just before SA.

HPLC chromatograms also exhibited peaks corresponding aliphatic acids as final products such as oxalic, glyoxylic, formic and maleic at retention time of 1.4, 1.6, 1.8 and 2.1 min, respectively. Fig. 7 shows that these acids were formed at the beginning of the treatment, they reach their maximum concentration then they are progressively destroyed. This maximum is obtained between 60-180 min for formic, glyoxylic and maleic acid and to 360 min for oxalic acid. Maleic acid comes from the destruction of aromatic intermediates, whereas oxalic acid is formed from the oxidation of longer chain carboxylic acids as maleic acid[22]. Oxalic and formic acid remains long time in solution due to the lower reactivity of radicals generated $^{\bullet}OH$ on this anode material towards aliphatic acid oxidation.

Decay kinetics of SA

The decay of SA in this trial was followed by HPLC where it displayed a well-defined peak with a retention time of 6.6 min. As can be seen in Fig. 8, the SA disappears after 480 min of treatment. The inset panel of Fig. 8 shows the pseudo-first-order kinetics followed by SA oxidation, with a rate constant of 8.3 10^{-3} min^{-1} (square regression coefficient, R^2 = 0.9931). The excellent linear correlation obtained suggests the production of a constant concentration of hydroxyl radicals from reaction (1) during electrolysis, which is much greater than that of SA near PbO_2 surface.

Proposed mineralization pathway

A plausible reaction pathway for SA mineralization in acid medium by anodic oxidation process is proposed in Fig. 9. Oxidation mechanism includes all oxidation by-products identified in the work and considers that the main oxidant is the hydroxyl radical generated at anode. The process is initiated by $^{\bullet}OH$ attack at the C(1) or C(3)-position of SA, breaking its to yield 2,6-dimethoxyhydroquinone and 3,4-dihydroxy-5-methoxybenzoic acid (3-O-methylgallic acid), respectively. However, with Liquid chromatography–mass spectrometry (LC/MS) analysis in our earlier investigations[18], it is only expected to be 3-O-methylgallic acid. Subsequently, it forms as quinone by dehydrogenation reaction with $^{\bullet}OH$. All these phenolic ring molecules can be oxidized and converted to ring cleavage small fragmented products which would be eventually give short chain aliphatic acids (maleic, glyoxylic and fumaric acids) by $^{\bullet}OH$ attack. Further oxidation of these products leads to oxalic and formic acids. Besides, it is proved in the earlier studies[23], that aliphatic acids are formed in the final step prior to CO_2 conversion, when phenolic compounds undergo the electrooxidation process. Finally, these short chain aliphatic acids were destructed resulting in a complete oxidation of SA.

4. CONCLUSION

The feasibility of SA removal by anodic oxidation using PbO_2 or BDD electrode was studied in bulk electrolysis under all conditions tested involving applied current from 8 to 120 mA cm^{-2} and SA concentration between 136 and 1100 mg O_2 L^{-1} COD. Both anodes have proved their great oxidation ability to remove SA from wastewaters and the oxidation rate increases with rising applied current density and initial SA concentration. The current efficiency increases with rising SA concentration and with decreasing applied current density. The performance of the BDD anode is always better than that of PbO_2, requiring shorter electrolysis time to reach overall mineralization, thus leading to remarkably higher current efficiency and lower specific energy consumption. These trends can be accounted for by the different nature of physisorbed hydroxyl radical generated on both electrodes and electro-catalytic properties of BDD anode.

Besides, electrochemical oxidation of SA on PbO_2 anode shows that the decay kinetics of SA follows a pseudo-first-order reaction. For SA degradation, 3-O-methylgallic acid and 2,6 dimethoxybenzoquinone are detected as aromatic intermediates, whereas a mixture of short linear carboxylic acids evolving to oxalic, maleic, glyoxylic and formic acids as final products are identified and quantified.

Acknowledgements

The authors would like to thank Prof. Mohamed BOUAZIZ, from Institut of Biotechnology-Sfax for his help in LC/MS analysis.

References

1 P. Canizares, J. Lobato, R. Paz, M.A. Rodrigo, C. Saez, Chemosphere, 2007, 67, 832.

2 S. Kallel Trabelsi, N. Belhadj Tahar, B. Trabelsi, R. Abdelhedi, J. Appl. Electrochem., 2000, 35, 5967.

3 C.A. Martínez-Huitle, M.A. Rodrigo, I. Sires, O. Scialdone, Chem. Rev., 2015, 115, 13362.

4 C.A. Martínez-Huitle, S. Ferro, Chem. Soc. Rev., 2006, 35, 1324.

5 I. Sirés, E. Brillas, M. A. Oturan M. A. Rodrigo, M. Panizza, Environ. Sci. Pollut. Res., 2014, 21, 8336.

6 O. Dridi Gargouri, Y. Samet, R. Abdelhedi, W. S. Africa., 2013, 39, 31.

7 M. Panizza, G. Cerisola, Chem. Rev., 2009, 109, 6541.

8 Y. Samet, L. Agengui, R. Abdelhedi, Chem Eng. J., 2010, 161, 167.

9 S. Ellouze, M. Panizza, A. Barbucci, G. Cerisola, T. Mhiri, S.C. Elaoud, J. Taiwan. Inst. Chem. E., 2016, 59, 132.

10 M. Hamza, R. Abdelhedi, E. Brillas, I. Sires, J. Electroanal. Chem., 2009, 627, 41.

11 L. Gherardini, P.A. Michaud, M. Panizza, C. Comninellis, N. Vatistas, J. Electrochem. Soc., 2001, 148, 78.

12 E. Brillas, C.A. Martínez-Huitle, Appl. Catal. B., 2015, 166-167, 603.

13 E. Guinea, C. Arias, P.L. Cabot, J.A. Garrido, R.M. Rodriguez, F. Centellas, E. Brillas, Water. Res., 2008, 42, 499.

14 M. Carbajo, F.J. Beltran, O. Gimeno, B. Acedo, F.J. Rivas, Appl. Catal. B., 2007, 74, 203.

15 D.E. Heredia, J.B. Torregrosa, J. Dominguez, J.R. Peres, Chemosphere, 2001, 45, 85.

16 O. Gimeno, M. Carbajo, M.J. Lopez, J.A. Melero, F. Beltran, F.J. Rivas, Water. Res., 2007, 41, 4672.

17 W. Gernjak, T. Krutzler, A. Glaser, S. Malato, J. Caceres, R. Bauer, A.R. Fernandez-Alba, Chemosphere, 2003, 50, 71.

18 O. Dridi Gargouri, B. Gargoui, S.K. Trabelsi, M. Bouaziz, R. Abdelhedi, Biochim. Biophys. Acta., 2013, 1830, 3643.

19 S. Garcia-Segura, E.V. dos Santos, C.A. Martínez-Huitle, Electrochem. Commun., 2015, 59, 52.

20 I. Sires, P.L. Cabot, F. Centellas, J.A. Garrido, R.M. Rodrıguez, C. Arias, E. Brillas, Electrochim. Acta., 2006, 52, 75.

21 Z. Wu, M. Zhou, Environ. Sci. Technol., 2001, 35, 2698.

22 B. Boye, M.M. Dieng, E. Brillas, Environ. Sci. Technol., 2002, 36, 3030.

23 B. Gozmen, M.A. Oturan, N. Oturan, O. Erbatur, Environ. Sci. Technol., 2003, 37, 3716.

Figures captions:

Fig. 1. Effect of current density on the variation of COD with (a_1 and b_1) electrolysis time and (a_2 and b_2) specific charge during the electrolysis of 540 mg O_2 L^{-1} COD of SA solutions in 0.5 M H_2SO_4. T = 30°C; (a_1 and a_2): AO-PbO_2; (b_1 and b_2): AO-BDD; j_{app}: (♦) 8; (■) 15; (▲) 60 and (□) 120 mA cm^{-2}.

Fig. 2. COD abatement vs. specific charge time during the electrolysis of SA solutions in 0.5 M H_2SO_4. (a) AO-PbO_2 and (b) AO-BDD. T=30 °C; j_{app} =15 mA cm^{-2} ; Initial COD concentration: (♦) 136; (▲) 280 (■) 540 and (□) 1100 mg O_2 L^{-1}.

Fig. 3. Comparison of the trend of COD during anodic oxidation of SA on (♦) PbO_2 and (◊) BDD anodes. Conditions: T=30 °C; j_{app} =15 mA cm^{-2}; pH = 1.8; COD_0= 540 mg O_2 L^{-1} .

Fig. 4. Current efficiency vs. time during anodic oxidation of SA solutions on (a) Ta/PbO_2 and (b) BDD anodes. T = 30◦C; j_{app} =15 mA cm^{-2}; Initial COD concentration: (♦) 136; (■) 280 (▲) 540 and (□) 1100 mg O_2 L^{-1}.

Fig. 5. LC-MS/MS Spectra (MS^1 and MS^2) of 3-O-methylgallic acid (a and b) and 2,6 dimethoxybenzoquinone (c and d) formed after 240 minutes of SA oxidation on PbO_2 anode. j_{app} = 15 mA cm^{-2}; pH = 1.8; T = 30 ° C.

Fig. 6. HPLC chromatograms after 240 min of anodic oxidation of 2 mmol L^{-1} SA at Ta/PbO_2 anode. j_{app} =15 mA cm^{-2} ; pH= 1.8; T= 30°C. **(1)** Carboxylic acids; **(2)** 3-O-methylgallic acid; **(3)** SA; **(4)** 2,6 dimethoxybenzoquinone.

405 **Fig. 7.** Evolution of the concentration of carboxylic acids detected during the anodic oxidation
406 of 2 mmol L^{-1} SA solutions in 0.5M H_2SO_4 on Ta/PbO_2 anode. j_{app} =15 mA cm^{-2} ; pH= 1.8;
407 T= 30°C. (●) Maleic acid, (∗) Glyoxylic acid, (×) Formic acid and (▲) Oxalic acid.
408
409 **Fig. 8.** SA decays with time during anodic oxidation of 2 mmol L^{-1} SA solution in 0.5 M
410 H_2SO_4 at Ta/PbO_2 anode. T = 30◦C; japp= 15 mA cm−2. The inset panel shows its kinetic
411 analysis assuming that the SA follows a pseudo-first-order reaction.
412
413 **Fig. 9.** Proposed reaction pathway of the electrochemical degradation of SA in acid medium
414 at Ta/PbO_2 or BDD electrodes.

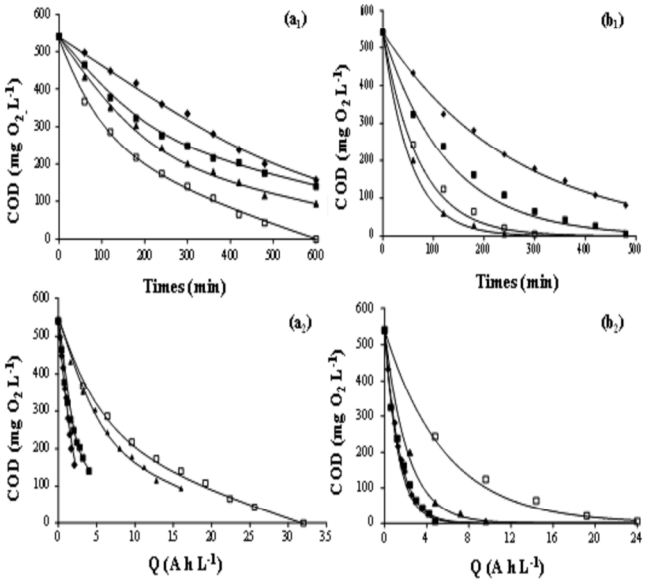

Fig. 1. Effect of current density on the variation of COD with (a1 and b1) electrolysis time and (a2 and b2) specific charge during the electrolysis of 540 mg O2 L-1 COD of SA solutions in 0.5 M H2SO4. T = 30◦C; (a1 and a2): AO-PbO2; (b1 and b2): AO-BDD; japp: (•) 8; (■) 15; (▲) 60 and (□) 120 mA cm−2.

1049x1484mm (120 x 120 DPI)

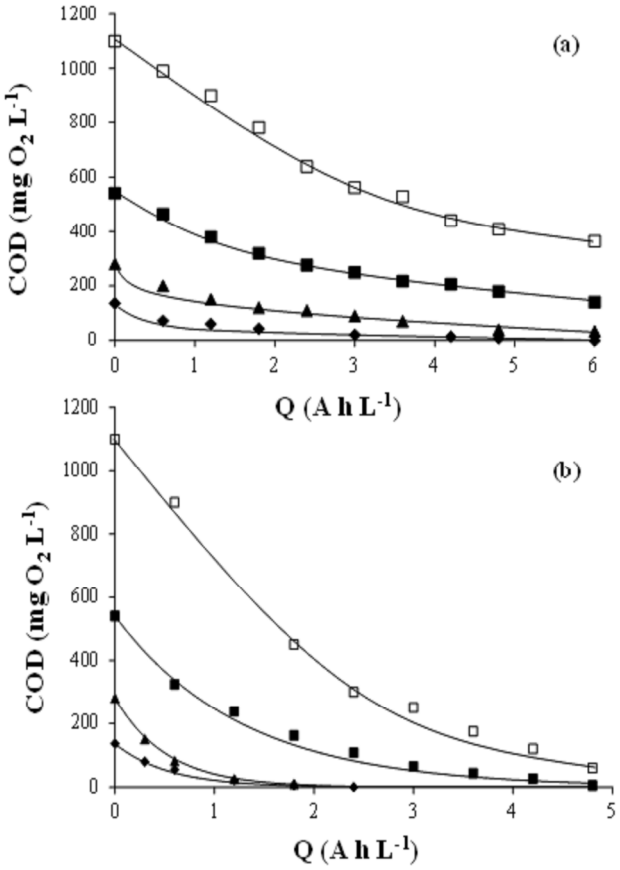

Fig. 2. COD abatement vs. specific charge time during the electrolysis of SA solutions in 0.5 M H2SO4. (a) AO-PbO2 and (b) AO-BDD. T=30 °C; japp =15 mA cm−2 ; Initial COD concentration: (•) 136; (▲) 280 (■) 540 and (□) 1100 mg O2 L-1.

1049x1484mm (120 x 120 DPI)

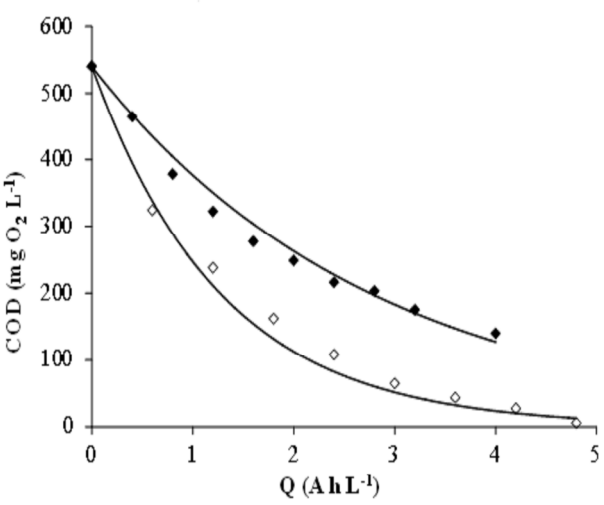

Fig. 3. Comparison of the trend of COD during anodic oxidation of SA on (•) PbO2 and (◊) BDD anodes. Conditions: T=30 °C; japp =15 mA cm−2; pH = 1.8; COD0= 540 mg O2 L-1 .

1049x1484mm (120 x 120 DPI)

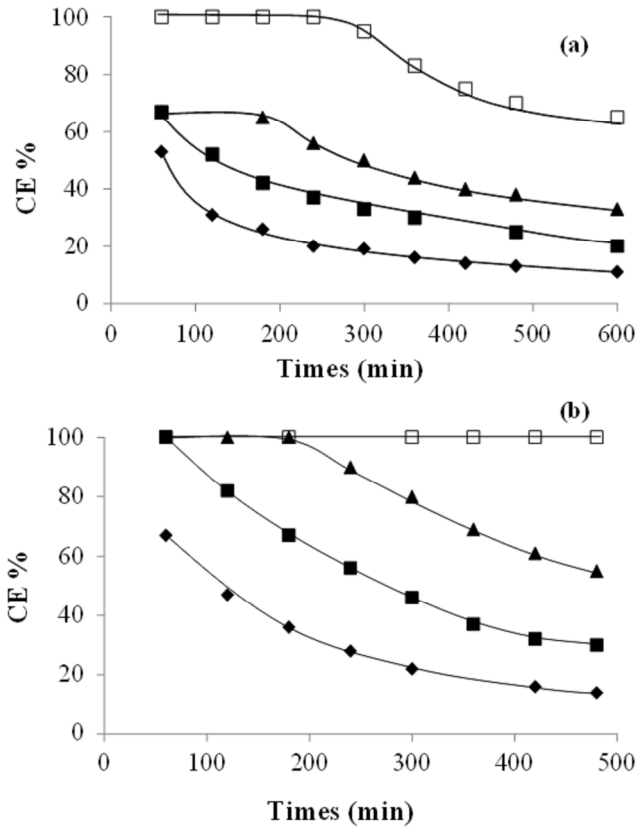

Fig. 4. Current efficiency vs. time during anodic oxidation of SA solutions on (a) Ta/PbO2 and (b) BDD anodes. T = 30◦C; japp =15 mA cm−2; Initial COD concentration: (•) 136; (■) 280 (▲) 540 and (□) 1100 mg O2 L-1.

1049x1484mm (120 x 120 DPI)

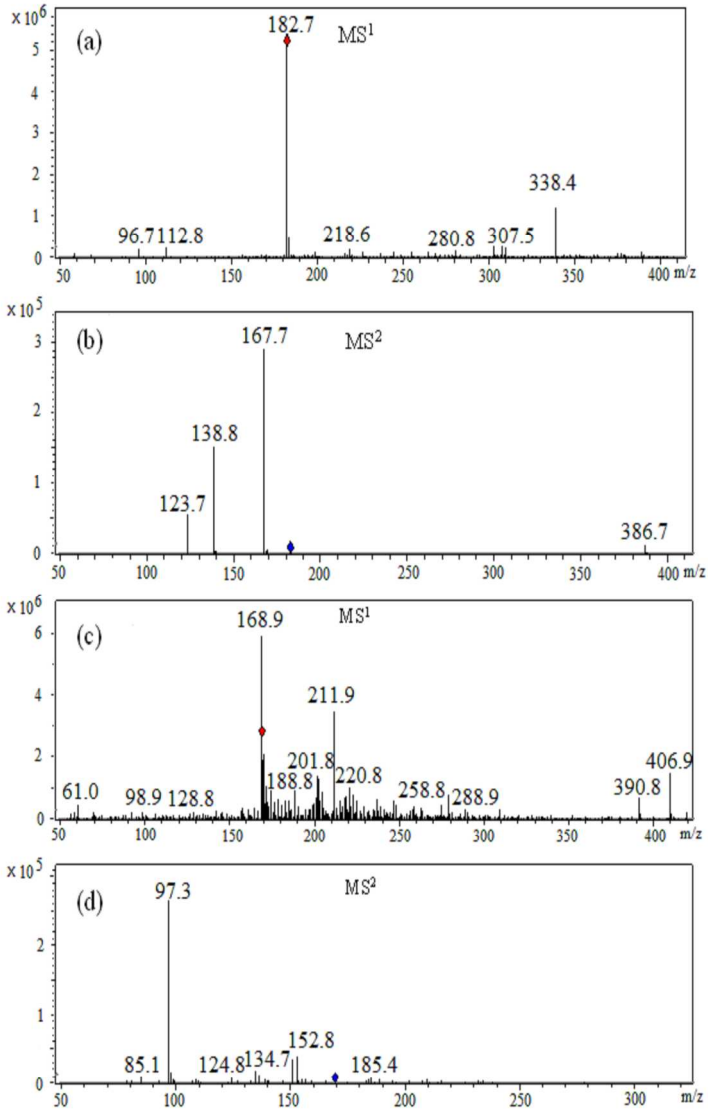

Fig. 5. LC-MS/MS Spectra (MS1 and MS2) of 3-O-methylgallic acid (a and b) and 2,6 dimethoxybenzoquinone (c and d) formed after 240 minutes of SA oxidation on PbO2 anode. japp = 15 mA cm-2; pH = 1.8; T = 30 ° C.

1049x1484mm (120 x 120 DPI)

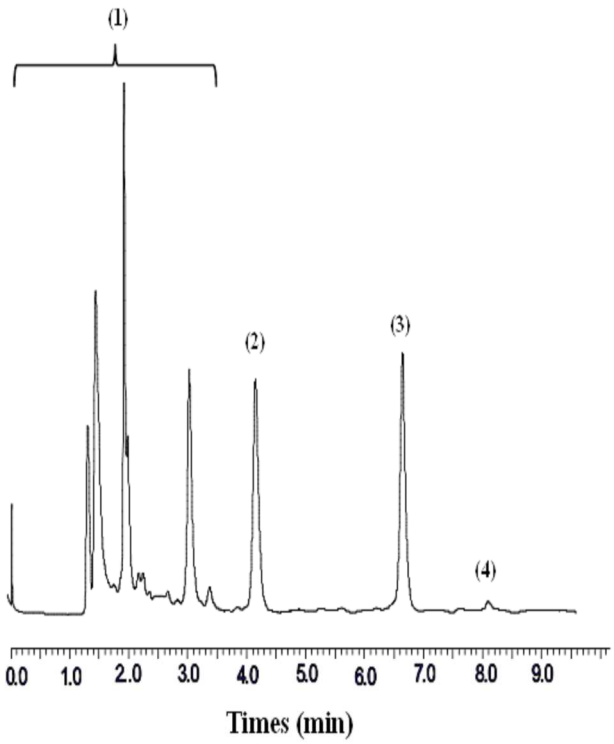

Fig. 6. HPLC chromatograms after 240 min of anodic oxidation of 2 mmol L-1 SA at Ta/PbO2 anode. japp =15 mA cm-2 ; pH= 1.8; T= 30°C. (1) Carboxylic acids; (2) 3-O-methylgallic acid; (3) SA; (4) 2,6 dimethoxybenzoquinone.

1049x1484mm (120 x 120 DPI)

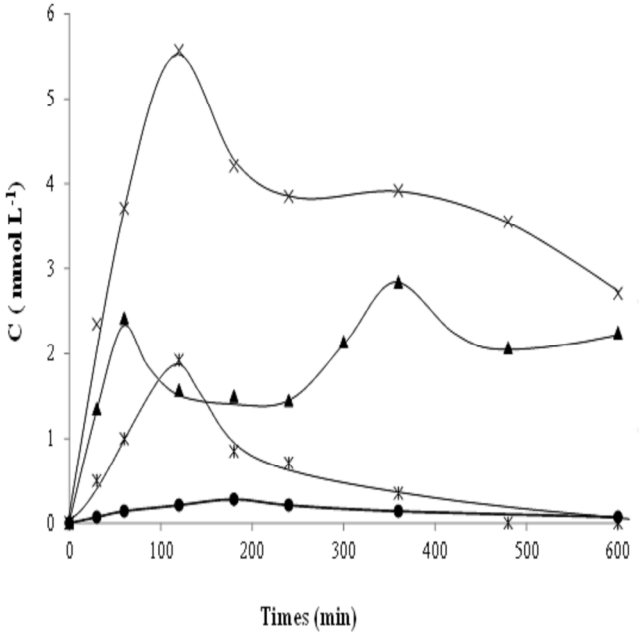

Fig. 7. Evolution of the concentration of carboxylic acids detected during the anodic oxidation of 2 mmol L-1 SA solutions in 0.5M H2SO4 on Ta/PbO2 anode. japp =15 mA cm-2 ; pH= 1.8; T= 30°C. (•) Maleic acid, (∨) Glyoxylic acid, (×) Formic acid and (▲) Oxalic acid.

1049x1484mm (120 x 120 DPI)

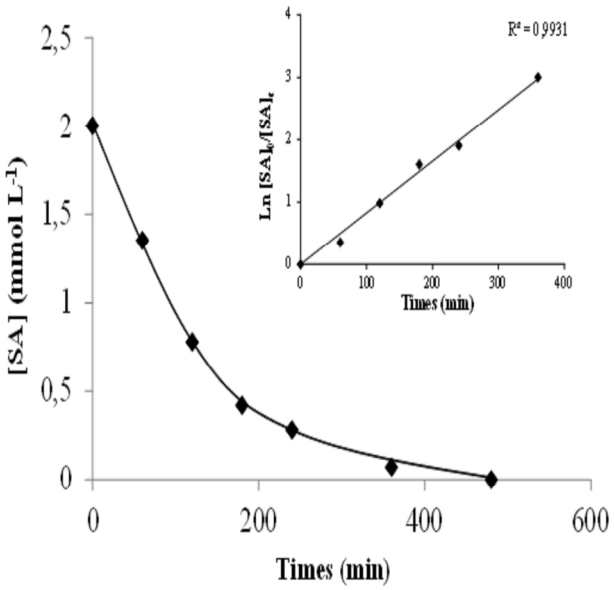

Fig. 8. SA decays with time during anodic oxidation of 2 mmol L-1 SA solution in 0.5 M H2SO4 at Ta/PbO2 anode. T = 30◦C; japp= 15 mA cm−2. The inset panel shows its kinetic analysis assuming that the SA follows a pseudo-first-order reaction.

1049x1484mm (120 x 120 DPI)

Table 1: COD removal (%), Current Efficiency (%) and Energy consumption (kWh (kg COD)$^{-1}$) evolution for 150 mL of 2 mmol L^{-1} SA solutions in 0.5 M H_2SO_4 of pH 1.8 at 30°C treated by anodic oxidation under selected condition.

Methods	j_{app} ($mA\ cm^{-2}$)	*After 60 min treatment*			*After 180 min treatment*			*After 480 min treatment*		
		COD removal	CE	Esp	COD removal	CE	Esp	COD removal	CE	Esp
AO-PbO_2	8	8	68	13.5	23	65	13.5	63	65	13.5
	15	14	63	40	40	60	41	68	38	71
	60	20	23	102	44	16	200	79	11	183
	120	32	18	220	60	11	280	92	6	419
AO-BDD	8	20	100	6.7	48	90	7.45	85	60	11.6
	15	40	100	10.05	70	70	14.83	99	37	28.06
	60	63	48	21.63	95	24	43.27	100	28	69.3
	120	55	20	51.92	88	11	94.41	100	7	173.1

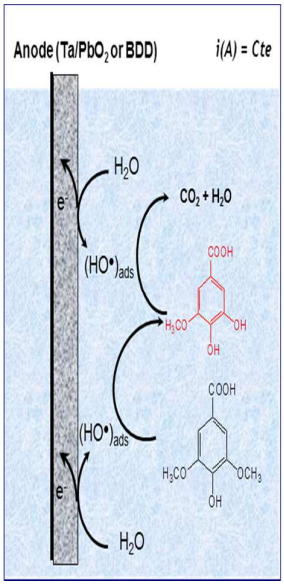

High oxidation power anodes (PbO_2 or BDD), lead to complete electrochemical removal of Syringic Acid under particulary experimental conditions.